

Anisotropic microhardness and crack propagation in epitaxially grown GaN films

This article has been downloaded from IOPscience. Please scroll down to see the full text article.

2000 J. Phys.: Condens. Matter 12 10241

(<http://iopscience.iop.org/0953-8984/12/49/324>)

View [the table of contents for this issue](#), or go to the [journal homepage](#) for more

Download details:

IP Address: 171.66.16.226

The article was downloaded on 16/05/2010 at 08:10

Please note that [terms and conditions apply](#).

Anisotropic microhardness and crack propagation in epitaxially grown GaN films

P Kavouras, Ph Komninou†, M Katsikini, V Papaioannou, J Antonopoulos and Th Karakostas

Department of Physics, Aristotle University of Thessaloniki, GR-54006 Thessaloniki, Greece

E-mail: komnhnoy@auth.gr

Received 29 September 2000

Abstract. The anisotropic character of microhardness of cubic and hexagonal GaN films epitaxially grown on silicon and sapphire, respectively, is investigated. A series of Vickers indentations demonstrate anisotropic indentation induced crack propagation in cubic GaN, whereas in the hexagonal material no cracks are formed for indentations with the same load. Directions of easy crack propagation are observed. A series of Knoop indentations is conducted in order to inspect the probable microhardness orientation dependence relative to the main crystallographic directions of films. The measurements reveal an orientation dependence of microhardness at room temperature only in hexagonal GaN films. The indentations are made with an angular interval of five degrees and the microhardness–orientation curve is obtained. The curve has a periodicity close to sixty degrees.

1. Introduction

During the past decade the vast majority of research in GaN films has been concentrated on their optoelectronic characteristics. In contrast, research on the mechanical properties has not drawn equal attention. A reason is that the growth of large GaN monocrystals is still a problematic issue. As a result classical methods for measurement of elastic constants are not applicable. A number of publications involve the determination of mechanical properties of GaN bulk crystals by nanohardness and conventional hardness testing [1, 2]. Due to the lattice mismatch and significant difference in thermal expansion coefficients between GaN films and the available substrates, the films are characterized by a large concentration of extended defects that affect their mechanical properties. Hence, it is becoming increasingly evident that research on the mechanical properties of GaN films will be needed for a more successful application of this semiconductor.

In this work two types of GaN film are investigated. One type is a cubic GaN film grown on Si by the electron cyclotron resonance plasma assisted molecular beam epitaxy (ECR-MBE) method, while the other type is a hexagonal GaN film grown on Al₂O₃ by metallorganic vapour phase epitaxy (MOVPE). The anisotropy of crack propagation in cubic GaN films is examined and correlated with the structure of the film with Vickers indenter geometry, while in the case of the hexagonal film no microcrack initiation was observed for the same indentation conditions. The anisotropic character of microhardness value is studied in both specimens but it is revealed only in the hexagonal polytype. A careful and systematic approach to the

† Corresponding author.

microhardness method is adapted, since this kind of measurement is influenced by indentation induced crack formation and the effect of the substrate [3].

2. Experimental details

Details on the growth conditions and characterization of the film have been published previously [4, 5]. The cubic GaN films were grown by ECR-MBE on (001) Si in two stages. First, a 30 nm buffer layer was deposited at 400 °C and then the 2 μm thick GaN epilayer at 600 °C was grown. The growth rate was 250 nm h⁻¹. The surface of the film shows a tile-like morphology. The tiles are oriented along the ⟨110⟩ directions. The hexagonal GaN film is nominally undoped and it was grown by MOVPE on (0001) Al₂O₃ substrate at 1050 °C. The 1.2 μm thick epilayer has a background carrier concentration of $n = 1 \times 10^{17} \text{ cm}^{-3}$.

The microhardness of the films was measured using a Knoop indenter (microhardness tester Anton Paar, MHT-10) in the range of 0.05–0.6 N for cubic GaN and 0.02–0.6 N for hexagonal GaN. The microhardness value H_K is calculated from the equation

$$H_K = 14\,229 \frac{P}{d^2} \quad (1)$$

where P is the load and d is the length of the long diameter of the indentation. The Vickers indenter geometry was used in order to inspect the microcrack propagation, since this indenter geometry induces microcracks for lower applied loads than the Knoop indenter. The surface roughness and the AFM micrographs were obtained using a Topometrix Explorer 2000 atomic force microscope.

The method of microhardness was used for this work for a number of reasons. Firstly, nanohardness is not applicable, since the roughness of the cubic and the hexagonal specimens is 200 Å and 45 Å respectively, as monitored by atomic force microscopy observations. This difference in roughness is inhibitory for the nanohardness use in both specimens, because the results would not be safely comparable. Secondly, the Knoop indenter, due to its geometrical configuration is appropriate for microhardness anisotropy detection [6].

In order to obtain reliable microhardness values in films, attention must be paid to the effect of the substrate. For this reason the microhardness of the substrate was also measured in the case of cubic GaN films, where the substrate is softer than the film. In this way, it is possible to deconvolute the measured microhardness of the film from that of the substrate. The basic idea relies on the fact that the measured microhardness of the film is a composite microhardness which depends on both the substrate and the film hardness. The extent that these two contributions affect the measured film composite microhardness is specified by a weighted law of mixture. Each contribution is analogous to the area over which the pressure from the indenter is exerted (area law of mixture). The deconvolution method used was originally developed by Jönsson and Hogmark [7] for the Vickers indenter and adapted to the geometrical configuration of the Knoop indenter by Torregrosa *et al* [8] and Iost [9]. Details of the analysis are given in the above references.

In the case of hexagonal GaN films, a microhardness anisotropy following the crystallographic anisotropy was revealed. The deconvolution method is not necessary in this case, because our purpose is to show the sinusoidal fluctuation in microhardness. The Knoop indenter was also used here, since the Vickers indenter requires the ratio of film thickness (t) over the indentation depth (d) to be greater than five ($t/d > 5$), for the case of softer film (GaN) on a harder substrate (Al₂O₃) [7]. In contrast, the Knoop indenter is specially made for microhardness measurements with low applied loads and low indentation depths, since the

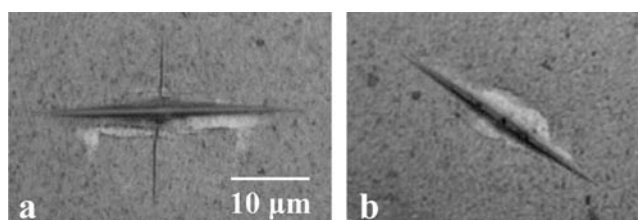


Figure 1. Optical micrographs of two Knoop indentations obtained with a load of 1.2 N. (a) Indentation print with the long diagonal parallel to the [110] direction with induced microcracks. (b) Indentation print with the long diagonal bisecting the $\langle 110 \rangle$ directions.

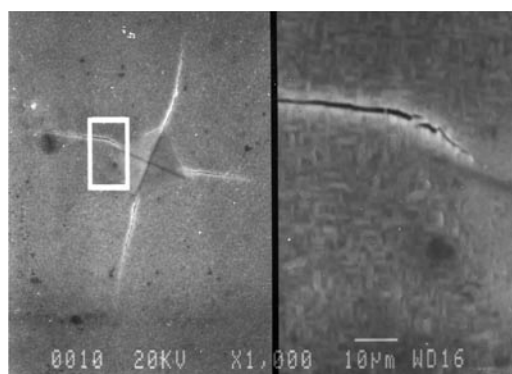


Figure 2. The diagonals of this indentation print form a 20° angle with the [110] directions. The frame is magnified five times more. The arrow indicates the microcrack bending.

indentation depth is 30 times smaller than the length of the long diameter of the indentation print. As a result, measurements with the Knoop indenter are more reliable than with the Vickers indenter in this case.

3. Results

3.1. Cubic GaN on (001) Si

Knoop microhardness measurements were conducted in order to measure the microhardness of cubic GaN grown on (001) Si. Observations reveal that above 0.6–0.7 N, microcracks emanate from the edges of the indentation and normal to the indentation's long diagonal, when it is parallel to the $\langle 110 \rangle$ directions (figure 1(a)). Indentation prints with the long diagonal bisecting the $\langle 110 \rangle$ directions showed a different behaviour. The absence of microcracks is clear (figure 1(b)) although the indentation load is the same as that of the indentation print in figure 1(a).

Microcrack propagation in this case was observed above 1.6 N applied load (figure 1). The length of the microcracks is proportional to the applied load until the value of 1.8–2.0 N, at which point the GaN film buckles and detaches from the Si substrate. This length does not depend on the duration of the indentation in the time scale of 1–180 s.

In order to observe this asymmetric pattern of microcrack propagation in a more systematic way, a Vickers indenter was used. Figure 2 illustrates the tendency of the microcracks to propagate parallel to the $\langle 110 \rangle$ directions, which we will call easy propagation directions

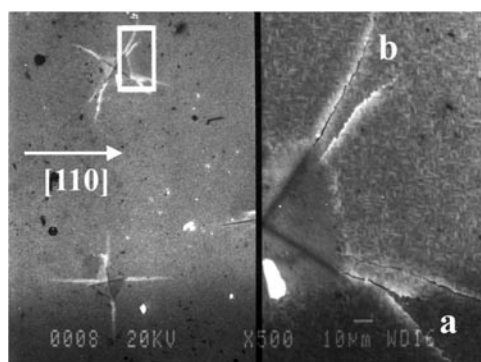


Figure 3. Vickers indentation with diagonals that bisect the $\langle 110 \rangle$ directions. In this case microcracks emanate from the indentation print corners by (a) one microcrack that is bifurcated or (b) two separated microcracks.

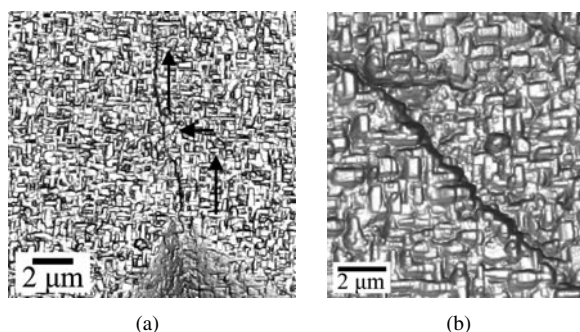


Figure 4. (a) A microcrack that propagates along a $\langle 110 \rangle$ direction with a step. The propagation is presented together with the tile-like surface morphology. The microcrack forms a step that is shown by arrows. This step is formed because the microcrack follows the borders of the tiles. (b) A microcrack stepped along the $\langle 110 \rangle$ directions is visible on the film surface having the tile-like morphology.

(EPDs). The bending is formed in order to align the microcrack parallel to the $[110]$ direction. When the indentation diagonals bisect the EPD, the microcracks bifurcate and follow the EPD (figure 3).

This preferential microcrack propagation along $\langle 110 \rangle$ directions is correlated with the characteristic tile-like surface morphology. As is shown from the atomic force microscopy images of figure 4, the surface morphology of the film has the characteristic tile-like appearance. The tiles are oriented along the $\langle 110 \rangle$ directions [4, 5]. The microcracks make their way through the film surface by separating these tiles. It must be stressed that although the microcrack of figure 4(b) seems to propagate along a $\langle 100 \rangle$ direction, it makes its way through the borders of the tiles by separating them. So, the propagation along $\langle 100 \rangle$ directions is achieved by steps parallel to the $\langle 110 \rangle$ directions. This microcrack pattern separates the more closely packed surfaces of GaN and therefore the planes of lower surface energy. This microcrack propagation pattern could be attributed to the indentation induced dislocation accumulation at the borders of the tiles. In this way the borders become sources of microcrack initiation. However, cleavage fracture should be also considered as another possible mechanism for the generation of this microcrack propagation pattern.

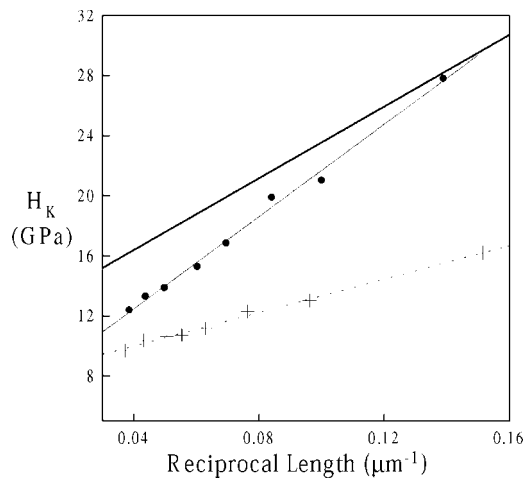


Figure 5. The deconvoluted microhardness of cubic GaN. (●) Experimental points of the composite microhardness (HK_C), (+) experimental points of substrate microhardness (HK_S). (a) Dotted line: linear fitting of the experimental substrate microhardness (HK_S). (b) Fine line: linear fitting of the modelled composite microhardness (HK_C). (c) Heavy line: the modelled film microhardness.

In order to compute the real microhardness value of the cubic GaN films, the deconvolution method mentioned previously is applied to the original microhardness data. The microhardness–load curve of the Si substrate was calculated from a (001) Si wafer. The load range used was 0.05–0.6 N, since microcrack free indentations could be obtained for both Si and cubic GaN. The extrapolated GaN microhardness was found to be equal to 11.6 GPa. The experimental composite hardness (GaN data) is in perfect agreement with the modelled one (figure 5), depicting that the deconvoluted microhardness value is reliable.

The composite microhardness reaches the values of the deconvoluted microhardness for large values of the reciprocal diagonal of the indentation or for indentation depths smaller than $\approx 0.22 \mu\text{m}$. This can be attributed to the fact that the shallower the indentation is, the less it is affected by the substrate. It is interesting to consider the specific film–substrate system. The film has a microhardness value of 11.6 GPa and the substrate a value of 8 GPa. As mentioned before, the microhardness measurements display no dependence on the substrate above the depth of $0.22 \mu\text{m}$, i.e. for $t/d \geq 9$. This is in agreement with the argument that the microhardness measurements are not influenced by the substrate for $t/d = 5$ for a film grown on a harder substrate and for $t/d = 14$ for a film grown on a softer substrate. In our case the film is slightly harder than the substrate, thus the ratio $t/d = 9$ is reasonable to exist between the two extreme values. Additionally, a complementary series of indentations were made, using the Knoop indenter geometry, in order to detect microhardness anisotropy. No microhardness anisotropy was observed in this case.

3.2. Hexagonal GaN on (0001) Al_2O_3

A series of Vickers indentations was performed in the same load range as for the cubic GaN. No microcrack propagation was observed. This fact leads to the assumption that hexagonal GaN has a higher fracture toughness than cubic GaN. The possible dependence of microhardness value on the orientation, with respect to specific crystallographic orientations, was studied for this polytype, with the Knoop indenter geometry. The measurements are presented in figure 6.

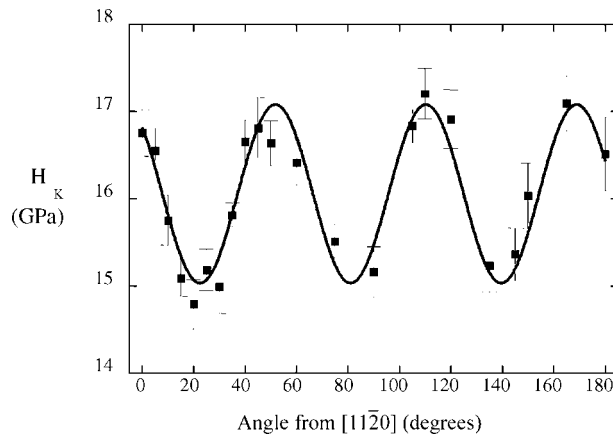


Figure 6. The sinusoidal fitting curve of the anisotropic microhardness together with the experimental points and the error bars. The microhardness value fluctuates with a period equal to 60° and an amplitude of 2 GPa.

The curve represents a series of measurements with a constant load of 0.5 N. This load value was chosen for two reasons: firstly, because it produces quite large indentations, thus the measurement errors are minimized; secondly, because the 0.5 N load resides clearly on the plateau of the microhardness–load curve, thus it is not affected by the indentation size effect. It is noticed that no indentation induced microcrack formation was observed in the range of 0.02–2.00 N, confirming the observations made with the Vickers indenter geometry.

The fitting curve of the experimental data points is also illustrated in figure 6. The curve is sinusoidal and exhibits a period equal to 60° . The positions of the microhardness maxima are related to specific crystallographic orientations of the film and are achieved when the large diagonal of the indentation is parallel to the $\langle 11\bar{2}0 \rangle$ directions of GaN. Accordingly, the microhardness minima are obtained when the indentation diagonal is rotated by 30° from the $\langle 11\bar{2}0 \rangle$ direction, namely when it is parallel to the $\langle 10\bar{1}0 \rangle$ direction. The fitting curve gives a mean value of microhardness equal to 16 GPa. This value is comparable to the measured value of hexagonal GaN on SiC that was found to be equal to 14 GPa [10] by microhardness measurements with a steel ball, without the use of a deconvolution method.

Measuring a lower microhardness value means that the material is more susceptible to plastic deformation along some specific orientations of the indenter. The material deformation is easier as shown in figure 6, when the indenter's large diagonal is parallel to $\langle 10\bar{1}0 \rangle$. The resolved shear stress (RSS) of a Knoop indenter can be calculated based on the assumption that its stress field is similar to that produced from an infinitely long flat punch of finite width subject to uniform pressure [11–13]. With this analysis the resolved shear stress on the basal plane should be zero. Thus, in the case of hexagonal GaN the possible slip systems are of the type $\langle 11\bar{2}0 \rangle \{1\bar{1}01\}$ and $\langle 11\bar{2}0 \rangle \{10\bar{1}0\}$. Therefore the anisotropy could be attributed to different activation of these slip systems as a function of the indentation orientation.

4. Conclusions

Anisotropic surface crack propagation, in cubic GaN films grown on (001) Si is studied using microindentation techniques. It is noted that the microcracks propagate on the surface of films along the $\langle 110 \rangle$ directions. When microcracks tend to propagate along $\langle 100 \rangle$, they bend and

finally are aligned parallel to the preferential propagation directions. The microcracks make their way through the GaN film by separating the tiles on the surface. Some small microcracks that seem to propagate along the $\langle 100 \rangle$ directions are stepped with the step facets being parallel to the $\langle 110 \rangle$ directions.

The Knoop microhardness of hexagonal GaN films grown on (0001) Al_2O_3 is measured and its dependence on the orientation with respect to the $\langle 11\bar{2}0 \rangle$ directions is revealed. The difference in microhardness between the maxima and minima of the H_K -angle curve is larger compared to the measurements' standard deviations. This anisotropic microhardness behaviour should be attributed to different activation of the possible slip systems as a function of the indentation orientation. Indentation induced microcrack formation was not observed for hexagonal GaN films in the same indentation conditions as those for the cubic polytype. This leads to the conclusion that hexagonal GaN grown on (0001) Al_2O_3 by MOVPE has higher fracture toughness than cubic GaN grown by ECR-MBE on (001) Si.

Acknowledgments

This work has been carried out under EU contract HPRN-CT-1999-00040, under GSRT contract No 99ED 320 and in a collaboration CNRS-NHRF contract No 8017. The samples were kindly provided by T D Moustakas (cubic GaN) and W T Masselink (hexagonal GaN).

References

- [1] Drory M D, Ager J W, Suski T, Grzegory I and Porowski 1996 *Appl. Phys. Lett.* **69** 4044
- [2] Nowak R, Pessa M, Suganuma M, Leszczynski M, Grzegory I and Porowski S 1999 *Appl. Phys. Lett.* **75** 2070
- [3] Li H and Bradt R C 1996 *J. Mater. Sci.* **31** 1065
- [4] Lei T, Moustakas T D, Graham R J, He and Berkowitz S J 1992 *J. Appl. Phys.* **71** 4933
- [5] Moustakas T D, Lei T and Molnar R J 1993 *Physica B* **185** 36
- [6] Marschall J and Milstein F 1994 *J. Mater. Sci.* **29** 3295
- [7] Jönsson B and Hogmark S 1984 *Thin Solid Films* **114** 257
- [8] Torrergosa S, Barrallier L, Roux L 1995 *Thin Solid Films* **266** 245
- [9] Iost A 1998 *Scr. Mater.* **39** 231.
- [10] Nikolaev V I, Shpeizman V V and Smirnov B I 2000 *Phys. Status Solidi* **42** 428
- [11] Hirsch P B, Pirouz P, Roberts S G and Warren P D 1985 *Phil. Mag. B* **52** 759
- [12] Roberts S G, Warren P D and Hirsch P B 1986 *J. Mater. Res.* **1** 162
- [13] Ebrahimi F, Gomez A and Hicks T G 1996 *Scr. Mater.* **34** 337